Published in final edited form as:
J Proteomics. 2011 December 21; 75(2): 410–424. doi:10.1016/j.jprot.2011.08.007.

Noise induced changes in the expression of p38/MAPK signaling proteins in the sensory epithelium of the inner ear

Samson Jamesdaniel, **Bohua Hu**, **Mohammad Habiby Kermany**, **Haiyan Jiang**, **Dalian Ding**, **Donald Coling**, and **Richard Salvi**[1]
Center for Hearing and Deafness, University at Buffalo, the State University of New York, Buffalo, NY 14214

Abstract

Noise exposure is a major cause of hearing loss. Classical methods of studying protein involvement have provided a basis for understanding signaling pathways that mediate hearing loss and damage repair but do not lend themselves to studying large networks of proteins that are likely to increase or decrease during noise trauma. To address this issue, antibody microarrays were used to quantify the very early changes in protein expression in three distinct regions of the chinchilla cochlea 2 h after exposure to a 0.5–8 kHz band of noise for 2 h at 112 dB SPL. The noise exposure caused significant functional impairment 2 h post-exposure which only partially recovered. Distortion product otoacoustic emissions were abolished 2 h after the exposure, but at 4 weeks post-exposure, otoacoustic emissions were present, but still greatly depressed. Cochleograms obtained 4 weeks post-exposure demonstrated significant loss of outer hair cells in the basal 60% of the cochlea corresponding to frequencies in the noise spectrum. A comparative analysis of the very early (2 h post-exposure) noise-induced proteomic changes indicated that the sensory epithelium, lateral wall and modiolus differ in their biological response to noise. Bioinformatic analysis of the cochlear protein profile using “The Database for Annotation, Visualization and Integrated Discovery 2008” (DAVID - http://david.abcc.ncifcrf.gov) revealed the initiation of the cell death process in sensory epithelium and modiolus. An increase in Fas and phosphorylation of FAK and p38/MAPK in the sensory epithelium suggest that noise-induced stress signals at the cell membrane are transmitted to the nucleus by Fas and focal adhesion signaling through the p38/MAPK signaling pathway. Up-regulation of downstream nuclear proteins E2F3 and WSTF in immunoblots and microarrays along with their immunolocalization in the outer hair cells supported the pivotal role of p38/MAPK signaling in the mechanism underlying noise-induced hearing loss.

Keywords

cochlea; sensory epithelium; Williams Syndrome transcription factor; E2F3; focal adhesion kinase; proteomics; noise-induced hearing loss; p38-MAP kinase

[1]Corresponding author: salvi@buffalo.edu, phone: 716-829-5310, fax: 716-829-2980, Center for Hearing and Deafness, University at Buffalo, the State University of New York, 137 Cary Hall, UB South Campus, Buffalo, NY 14214.

Introduction

Prolonged exposure to high intensity noise in occupational or recreational settings is a major hearing health care problem. Worldwide, noise exposure accounts for roughly 16% of cases of hearing loss in adults [1] and among combat personnel, the percentage rises to 50% [2]. Exposure to loud noise causes a number of pathological changes in the cochlea resulting in elevated hearing thresholds. Noise exposure can adversely affect all three regions of the cochlea (Fig. 1), the organ of Corti, the lateral wall and the spiral ganglion neurons (SGN) [3–7]. Much of the research on noise-induced hearing loss (NIHL) has focused on the sensory hair cells in the organ of Corti where auditory transduction occurs [8–11], but there is growing awareness that the SGN and lateral wall of the cochlea are adversely affected by noise [7, 12]. The organ of Corti contains two types of sensory hair cells, outer hair cells (OHC) and inner hair cells (IHC). The OHCs, which are electromotile, act as a cochlear amplifier enhancing the sound-induced vibration of the basilar membrane [13]. The IHC, which make synaptic contact with 95% of SGN, play a major role in converting sound into neural activity and relaying this information through the auditory nerve fibers to the central auditory system. The hair cells, particularly OHCs, are considered to be the most susceptible to noise-induced damage.

Three modes of hair cell death have been reported in the inner ear - necrosis, apoptosis [9, 14], and an atypical mode of cell death featuring loss of plasma membrane in the basal pole of the OHC [15]. The molecular mechanisms that regulate the balance of cell death and cell survival in the inner ear are not completely understood, but there is growing awareness that mitogen-activated protein kinases may be important. p38/MAPK (Mapk14), a stress-activated member of the family of mitogen-activated protein kinases, is an importing important signaling protein that links activity at the cell membrane to downstream signaling in the nucleus. Cellular processes in which p38/MAPK participates are numerous and include inflammation, cell cycle regulation and apoptosis [16]. p38/MAPK can be activated by a diverse spectrum of environmental factors and endogenous stimuli which include Fas-mediated pathways [17] and focal adhesion signaling [18]. Inhibitors of p38/MAPK have been shown to confer protection to the inner ear from stress induced by noise [19] and the ototoxic antibiotic, gentamycin [20].

Williams syndrome transcription factor (WSTF) and E2F3 are two of the many signaling proteins downstream of p38/MAPK. WSTF (Baz1b) is a nuclear signaling protein that modulates transcription through chromatin remodeling. Phosphorylation of serine-158 on WSTF is required for vitamin D-dependent transcription [21]. E2F3 is a transcription factor involved in cell cycle regulation and induction of apoptosis. E2F3 activity is repressed by binding of the retinoblastoma protein (Rb). Hyperphosphorylation of Rb by p38/MAPK and cell cycle dependent protein kinases causes the release of Rb and transcriptional activation of E2F3 target genes [22].

Although several groups have identified protein changes associated with NIHL using Western blots and immunolabeling [12, 23, 24], these methods do not lend themselves to studying large networks of proteins that are likely to increase or decrease during noise trauma. In order to provide a broad overview of the very early protein expression changes associated with NIHL, we used antibody microarrays to investigate proteomic responses [25, 26] to acoustic overstimulation in three discrete regions of the chinchilla cochlea, viz. sensory epithelium, lateral wall and the modiolus containing the SGN. Importantly, an early two hour time-point was chosen to identify the initial proteomic responses that precede the noise-induced permanent shift in hearing threshold and loss of hair cells. Our results indicate that intense noise increased the levels of focal adhesion kinase phosphorylated on tyrosine-577, WSTF, diphosphorylated p38/MAPK and increased expression of E2F3.

Collectively, these results suggests that the sensory epithelium responds to noise through p38/MAPK signaling involving regulation of focal adhesion junctions in stereocilia and in the apical aspects of hair cells.

Materials and methods

Animals

Long-tailed chinchillas (C. lanigera) weighing from 450 to 750 g were used for these experiments because there is an extensive literature dealing with the anatomical, physiological and behavioral consequences of NIHL in this species and because their hearing range is comparable to that of humans [27–29]. The animals were maintained in a temperature-controlled room with a 12-h light/dark cycle and allowed free access to food and water. The experimental protocol was reviewed and approved by the University at Buffalo Institutional Animal Care and Use Committee. The animals were handled and treated according to guidelines established by the National Institutes of Health and the Institutional Animal Care and Use Committee at the University at Buffalo.

Reagents

All reagents were purchased from Sigma Aldrich Chemical Company (St. Louis, MO) unless noted otherwise.

Noise exposure

Awake chinchillas were exposed to 0.5–8 kHz bandpass noise at 112 dB SPL for 2 h. The signal was generated by a real time signal processor (Tucker Davis Technologies, TDT-RP2.1, Alachua, FL), amplified by a power amplifier (Samson, Servo 300) and delivered to an acoustic driver (2445J, James B. Lansing Sound Inc. North Ridge, CA) equipped with an exponential horn (2360T, JBL). Noise level was measured using a Larson Davis Laboratories 824 sound level meter equipped with a ½ inch condenser microphone (Larson and Davis 2540) and calibrated with a Larson Davis Laboratories CA250 calibrator.

Distortion product otoacoustic emissions (DPOAEs)

Cubic distortion product otoacoustic emission amplitudes, a highly sensitive measure of OHC function, were measured in awake, restrained animals as previously described [25, 30]. The two tones, f1 and f2, were presented at intensities where L2 = L1 – 10 dB and with f2/f1 = 1.2. DPOAE input/output functions were measured at L1 levels ranging from 80 to 25 dB SPL in 5 dB increments. F2 was varied from 4 to 16 kHz in half octave increments. Two IHS-3738 high frequency transducers (Intelligent Hearing System, Miami, FL, USA) were used to deliver the primary tones to the ear via flexible tubes. Sound pressure levels were measured at the cubic difference frequency (2f1-f2) using a model ER10B+ probe microphone (Etymotics Research, Inc., Elk Grove Village, IL) and hardware and software from Smart Distortion Product Otoacoustic Emission System version 4.53 (Intelligent Hearing Systems). The output of the microphone was sampled at 40 kHz over a period of 204 ms. The spectrum of each sweep was computed and averaged over 32 sweeps. The noise floor was measured in a 24 Hz band surrounding 2f1-f2.

Cochleogram

As described previously, chinchillas were anesthetized by CO_2 inhalation until there was no response to a toe pinch and then decapitated [25, 31]. The temporal bones were quickly removed, the round and oval windows were opened and the cochleae perfused with 10% buffered formalin (Fisher Scientific, Fair Lawn, NJ, pH 7, 40 °C) through the round window and subsequently immersed in fixative for 3 h. Specimens were then stained with Harris'

hematoxylin solution, dissected and mounted in glycerin on a glass slide. The number of missing IHC and OHC were counted over 0.24 mm intervals from apex to base using a light microscope (400×) [32]. Percent hair cell loss was plotted as function of percent total distance from the apex and the data used to construct a cochleogram. Percent distance along the length of the cochlea was related to frequency using a frequency-place map [33].

Sample preparation for microarray

Animals were anesthetized with CO_2 and decapitated 2 h after the noise exposure as previously described [25]. Cochlear tissue from the sensory epithelium (sensory), lateral wall (vascular) and modiolus (neural) was dissected separately from four chinchillas (Fig. 1). The bony shell was removed carefully without damaging the lateral wall and the whole cochlea was dissected out. Then the modiolus containing the spiral ganglion cells was gradually detached from the sensory epithelium from the apex to the base. Finally the lateral wall tissue was separated from the sensory epithelium. The tissue from each region was pooled from all four animals for analysis. The tissue was homogenized in a lysis buffer supplemented with protease inhibitors, phosphatase inhibitors and benzonase supplied with the antibody microarray (Sigma, St. Louis, MO). Homogenization was performed on ice in Kontes 1.5 ml homogenization tubes with fitted pestles using a 50% duty cycle (20 s pestle rotation / 20 s off) with a four cycle repetition. Homogenates were centrifuged at 10,000×g for 10 s and pellets were discarded. Protein concentration of the supernatant was determined using the Bradford assay [34] and adjusted to 1.5 mg/ml. Cy3 or Cy5 dyes (4,000 U, GE Healthcare) with N-hydroxysuccinimide active linkers were resuspended in 50 μl of 0.1 M carbonate-bicarbonate buffer (pH 9.6) and 7.5 μl of dye was added to the 100 μl protein sample (150 μg). The reaction was allowed to proceed for 30 min at room temperature after which labeled protein was separated from free dye by gel filtration on Sephadex G25 spin columns (Sigma). Protein concentration was again determined by the Bradford assay and dye incorporation was determined spectrophotometrically using extinction coefficients for Cy3 and Cy 5 of 0.15 μM^{-1} cm^{-1} at 552 nm for Cy3 and 0.25 μM^{-1} cm^{-1} at 650 nm for Cy5. Molar dye:protein ratios were calculated assuming an average protein molecular weight of 60,000 Da. To optimize the signal to noise ratio, labeling was repeated as necessary to achieve a molar dye/protein ratio > 2 [25].

Antibody microarray assay

A broad spectrum antibody microarray – XPRESS Profiler 725 kit (Sigma) spotted with 725 antibodies representing proteins involved in a variety of biological pathways, was used to profile the expression of proteins in three discrete regions of the cochlea [Note: More detailed information on the array can be found on the manufacturer's web site: www.sigma.com/xp725]. Samples from the noise exposed group were mixed with their respective controls (each labeled with opposite dyes) and applied simultaneously at equal protein concentrations of 30 μg/ml on arrays. To control for differences in labeling stoichiometry, a dye-swapping paradigm was used [35]. For each experiment, two slides spotted with antibodies were incubated with labeled protein samples for 0.5 h each at room temperature. The first slide was incubated with Cy3-labeled control sample mixed with Cy5-labeled noise exposed sample. A second identical slide was incubated with the opposite labeling scheme. Fluorescent signal intensities from the binding of Cy3- or Cy5-labeled protein were recorded for each antibody spot using a GenePix Professional 4200A Microarray Scanner (Molecular Devices Corporation, Sunnyvale, CA).

Data analysis

Background corrected fluorescence of the antibody spots was normalized using GenePix Pro 6.0 – Acuity 4.0 microarray informatics software (Molecular Devices). In this process the fluorescent values for each spot were adjusted by a multiplier so that the mean F532 / F635

values were equal to 1. All spots that either showed an uneven distribution or a negative signal to noise ratio were rejected from further analysis. Fold changes in fluorescence for each microarray slide were calculated from the arithmetic means of duplicate spots for each antibody. A linear regression analysis was performed on the fold changes of slide 1 and slide 2 by forcing the slope to pass through 0. The data points that were within the 95% prediction band (GraphPad Prism 5, La Jolla, CA) were included in further analysis. The geometric mean of the fold changes obtained from slide 1 and slide 2, which met the above criteria, was used to represent the expression levels of the proteins relative to control. Fold changes obtained from three biological repeats were averaged and ranked.

Bioinformatics analysis

Proteins that met the further criteria of fold change (noise exposed/control) < 0.8 or >1.2 were analyzed with bioinformatics software to systematically extract the involvement of specific signaling pathways in NIHL. The Database for Annotation, Visualization and Integrated Discovery 2008 (DAVID - http://david.abcc.ncifcrf.gov) was used for analyzing the data gathered from the high-throughput proteomic assays [36]. Gene symbols of the proteins that met our selection criteria were uploaded and analyzed using the text and pathway mining tools which classified the proteins based on their functional associations. Scientific literature on three different species (mouse, rats and humans) were used as background for the analysis. The clustering tool was employed to group related functional annotations. GNCPro software from SABiosciences (http://gncpro.sabiosciences.com) was used for network analysis.

Immunocytochemistry

Animals were sacrificed and the cochleae were fixed with 10% buffered formalin. The cochleae were dissected in 10 mM phosphate buffered saline (PBS) and the sensory epithelia were collected. The tissue was permeabilized with 0.2% Triton-X-100 in 10 mM PBS for 30 min and then incubated in a blocking buffer (Blocker™ Casein in PBS, Pierce Chemical Company, Rockford, IL) for 30 min at room temperature. Specimens were incubated overnight at 4 °C with either of three primary antibodies: anti- FAK p-Tyr577, rabbit polyclonal antibody against focal adhesion kinase phosphorylated on tyrosine 577 (Invitrogen - Life Technologies Corp., Carlsbad, CA, 1:200 in PBS), monoclonal anti-E2F3, (Sigma, 1:200 in PBS), or rabbit anti-C-terminal Williams syndrome transcription factor (anti-WSTF, Sigma, 1:200 in PBS). Unbound antibody was removed with three washes with 10 mM PBS. The tissues were then incubated with Alexa Fluor® 488 goat anti-mouse or anti-rabbit IgG (H+L) (Invitrogen Ind., 1:1000 in PBS) for 2 h, washed three times with PBS and then counterstained with propidium iodide (5 μg/ml in PBS) for 10 min. Specimens were mounted on slides containing antifade medium (Prolong Cold antifade reagent, Invitrogen) and examined using a Zeiss LSM 510 META (Carl Zeiss, Oberkochen, Germany) confocal microscope [37].

Nuclear protein and plasma membrane enrichment

Many of the proteins that underwent a noise-induced change in the sensory epithelium were nuclear proteins. Hence, to facilitate validation by immunoblotting methods, nuclear proteins and plasma membrane proteins from chinchilla cochleae were enriched using a modified protocol of Widnell and Tata [38]. Two cochleae were pooled and homogenized at 4 °C in 100 μl medium that contained 0.32 M sucrose and 3 mM $MgCl_2$. Kontes glass micro-homogenizers were used with a 10 s rotation followed by a 20 s extraction which was repeated 4 times. The homogenate was centrifuged at 800×g for 10 minutes and supernatant was removed and frozen in liquid nitrogen. The pellet was resuspended in 100 μl homogenizing medium and centrifuged again at 800×g for 10 minutes. The second supernatant was discarded and the pellet was extracted for 30 minutes in 60 μl of RIPA

buffer (Pierce) containing 5 mM EDTA, protease and phosphatase inhibitors (Pierce). The extracted nuclear proteins and plasma membrane proteins were collected after centrifugation at 14,000×g for 10 minutes. Protein concentration was determined using the Bradford assay.

Immunoblotting

Specificity and antigenicity of chinchilla cochlear proteins were assessed by immunoblotting [39]. Briefly, proteins from the nuclear and plasma membrane enriched fraction as well as the supernatant fraction were separated on 4–12 % gradient NuPage gels (Invitrogen), transferred to polyvinylidene difluoride (PVDF) membranes, blocked with 0.1% I-Block (Applied Biosystems, Foster City, CA) and probed with antibodies against WSTF (1:500), E2F3 (1:500) and v-Src (Calbiochem, 1:20) using chemiluminescence (Pierce Chemical Co., Rockford, IL). A Fuji model LAS 1000 imaging system (Stamford, CT) was used to visualize gel bands. Background corrected bands (NIH Image J software) were normalized against bands obtained by stripping the membrane with 25 mM glycine (BioRad), pH 2.0, 1% lauryl sulfate (Fisher Scientific) and reprobing with an antibody against actin (Millipore, Billerica, MA).

Results

Physiological measure of noise-induced permanent hearing loss

The mean (n = 10) amplitudes of the distortion products at 4, 8 and 16 kHz dropped to the noise floor 2 h after noise exposure confirming that the exposure induced a significant loss of OHC function in all animals used in the proteomic experiments (Fig. 2). To determine the extent of permanent damage from this exposure, we measured mean (n =3) distortion products for three additional animals over a 28 day period. The amplitudes of the distortion products at 8 and 16 kHz were at the level of the noise floor 1 day after noise exposure and remained there even after 7 days. There was a partial recovery after 28 days which was relatively small at 16 kHz (Fig. 3, right panel) and somewhat greater at 8 kHz (Fig. 3, left panel). Nevertheless the amplitudes were 10 – 20 dB less than the baseline levels suggesting a permanent threshold shift (PTS) induced by the noise exposure.

Anatomical measure of noise-induced permanent hearing loss

Cochleograms were constructed for the left and right ear of three chinchillas allowed to survive for 28 days following the exposure. This later time-point was chosen to quantify the long-term histopathologies as quantification of hair cell loss at 2 hours is unlikely to reflect the extent of permanent damage from this noise exposure. To summarize the histological results, a mean (n = 3, which included the averaged data from left and right cochlea) cochleogram showing the percentage of missing OHC and IHC was constructed for three noise exposed chinchillas (Fig. 4, percent distance from apex on lower abscissa; corresponding frequency on upper abscissa). Significant loss of both OHCs and IHCs was observed 28 days after noise exposure. OHC loss was widespread. Mean OHC loss ranged from 60–80% in the basal half of the cochlea (50–100% distance from apex) and gradually declined from approximately 60% OHC loss near the middle to less than 20% OHC loss near the apex. IHCs were more resistant to noise than were OHCs. IHC loss occurred mainly from 55–85% distance from the apex; the maximum IHC loss was approximately 40% at 75% distance from the apex. Left and right cochleae sustained comparable amounts of damage in all animals (data not shown). Together with the physiological data, the results confirmed that the noise paradigm used in this study was sufficient to cause a permanent threshold shift and substantial loss of OHC in the basal half of the cochlea. Hence the early proteomic changes observed in this study at 2 h post exposure likely represent upstream changes that in due course contribute to a permanent shift in the hearing threshold and significant loss of OHC.

Cochlear protein expression profile after noise exposure

To gain insight into the early changes in protein signaling pathways leading to permanent hearing loss, we performed a proteomic analyses 2 h after noise exposure using the same antibody microarrays that were used in our earlier proteomic studies of the inner [25, 26]. The specificity of the antibody microarray was initially assessed by immunoblotting chinchilla cochlear proteins with several representative antibodies. Detection of sharp bands of MAPK and Receptor Interacting Protein, at expected molecular weights, confirmed the specificity of spotted antibodies on the array (data not shown). During the microarray analysis, of 725 antibodies spotted on each array, we rejected the spots that did not produce uniform fluorescence above background in each of three biological repeats. After elimination of low level spots that represent absence of protein in cochlear samples or lack of antibody recognition of chinchilla proteins, further analysis was performed on 584 proteins from sensory epithelium (containing sensory and supporting cells), 392 proteins from lateral wall (containing cells that regulate ion balance and vascular supply) and 569 proteins from the modiolus (containing neurons, supporting and vascular cells in a bony spiral capsule). Histograms of fold changes for each tissue approximated a Gaussian distribution (Fig. 5). The range of fold changes, 0.7 to 1.4 fold, was similar for each tissue and fold changes were distributed around a mean fold value of 1 representing no change. However, the histogram for the modiolus was broader than for the lateral wall or the sensory epithelium indicating that noise may induce larger increases and decreases in neural proteins than in sensory or lateral wall proteins. An analysis of the distribution of the proteomic changes between these three discrete regions of the cochlea was done by plotting the fold changes of individual proteins from two different regions (e.g., sensory epithelium vs. lateral wall, Supplementary Fig. 1). No significant correlation between any two pairs of cochlear tissues was observed. This comparative analysis suggests that the protein levels may be regulated differently for each of the regions. The noise-induced protein fold changes for all detected proteins from the three cochlear regions have been presented in the supplementary data (Supplementary Table. 1). Importantly, the detected proteins in Supplementary Table 1 represent the most comprehensive profile of proteins present in the lateral wall, organ of Corti and modiolus of the chinchilla cochlea. Many of these proteins have not been detected before in the cochlea and therefore provide a trove of useful, new information.

Proteomic changes in the sensory epithelium

Noise induced an increase in 7 proteins (FAK p-Tyr577, E2F3, hMps1, serine threonine protein phosphatase 1b, activated p38/MAPK, WSTF and Fas) in the sensory epithelium that matched our criteria for increased or decreased expression (fold change > 1.2 or < 0.8). None of the noise-induced decreases in expression for sensory epithelium met this criterion. Analysis using NIH-DAVID indicated involvement of the Fas-induced mitochondrial death pathway mediated by p38 mitogen-activated protein kinase (2 proteins, $p < 0.001$), response to endogenous stimulus (3 proteins, $p < 0.01$) and response to stress (3 proteins, $p < 0.05$). The functional annotations associated with this data set were grouped into clusters based upon their functional similarities. An enrichment score is used to rank the biological significance of the clusters, where a higher enrichment score implies that the data set is more enriched with the proteins associated with that particular functional group. Cluster analysis indicated that the cluster which included tyrosine kinase activity (3 proteins, ($p <0.01$), and serine / threonine kinase activity (3 proteins, $p < 0.05$) had an enrichment score of 1.32, while the cluster which included 4 proteins and important functional annotations like response to endogenous stimuli and response to stress had an enrichment score of 0.97. Among the KEGG pathways associated with this data set, 2 proteins (FAK p-Tyr577 and serine threonine protein phosphatase 1β) were involved in focal adhesion and 2 other proteins (p38/MAPK, activated and Fas) were involved in MAPK signaling pathway. Network analysis using GNCPro software from SABiosciences indicated 5 of the 7 proteins

that changed in the sensory epithelium were involved in a network that also included Src (Fig. 6). This network is generated by searching the database for previous publications on interactions between these proteins under ten different categories. Multiple interactions between many of the proteins suggest that the noise-induced changes in these proteins might be inter-related and are more likely to reflect the underlying biological mechanism. Overall, the analysis of proteomic changes indicates the initiation of noise-induced cell death process in the sensory epithelium.

Proteomic changes in the lateral wall

Noise induced a decrease in the expression level of 4 proteins (E2F3, tropomyosin, CD146 and hnRNPA1) that matched the selection criteria in the lateral wall. Bioinformatics analysis using DAVID did not point out any common functional annotations. The noise-induced decrease in E2F3 might contribute to the development of NIHL as E2F3 is known to have an important role in apoptosis. No major pathways were identified. This indicates that the noise-induced proteomic changes in the lateral wall are smaller than those in other regions of the cochlea.

Proteomic changes in the modiolus

Noise induced an increase in 4 proteins (aurora B, BID, HDAC10 and ADAM17) and a decrease in 7 proteins (cytokeratin 8 12, PRMT1, serine threonine protein phosphatase 2 A/B, NG2, brain nitric oxide synthase, DEDAF and plakoglobin) that matched the selection criteria in the modiolus. These proteins were analyzed using DAVID bioinformatics resources. Signal transduction ($p=0.0072$) and cell death ($p=0.0099$) were among the important functional annotations identified with the involvement of 6 and 3 proteins in each of these categories respectively. Cluster analysis of functional annotations indicated that a cluster representing cell death/development had an enrichment score of 0.92. On the whole, the proteomic changes observed in the modiolus suggest the predominance of an apoptotic response to noise exposure in the neural tissue.

Immunolocalization in organ of Corti

Three proteins of interest, E2F3, FAK p-Tyr577, and WSTF, were immunolocalized in the inner ear 2 h after noise exposure. These three served as representatives of a larger set of proteins whose noise-induced changes were detected by the antibody microarray assay. In normal cochlea, E2F3 staining was barely detectable above background in OHC, IHC (OHC and IHC shown in Fig. 7D) and supporting cells (Fig. 7A). Likewise, E2F3 was barely detectable in IHC in noise-exposed cochleae (Figs. 7B and 7C). In contrast, immunolabeling revealed strong expression of E2F3 in OHC nuclei in regions damaged by noise exposure. The noise-induced expression pattern of E2F3, primarily in OHC, is consistent with the finding of significant OHC loss at 28 days post-exposure (Fig. 4) and large reductions in DPOAE amplitude at 2 h post-exposure (Fig. 2). Nuclear condensation is a marker of apoptosis in NIHL [14]. E2F3 is expressed in OHC where nuclear condensation has begun, but not in OHC with fully condensed nuclei (Fig. 7C, F). The number of OHC stained with E2F3 and the intensity of E2F3 staining decreased with distance from the site of the lesion. Overall, increased expression of E2F3 in noise damaged OHC is consistent with the findings of the antibody microarray, which indicated an increase in expression level in the sensory epithelium after noise exposure.

Immunolabeling of focal adhesion kinase phosphorylated on Tyr-577 revealed strong expression in the phalangeal processes of Deiters' cells and in the apical region of the pillar cells and, to a much lesser degree, in OHC in the normal cochleae (Fig. 8A, 8B and 8C). In these cochleae, the nuclei of IHC and Hensen's cells also displayed strong immunoreactivity. Following the noise exposure, a remarkable increase in the

immunoreactivity of FAK p-Tyr577 was observed in the stereocilia of OHC in the noise-damaged regions in the organ of Corti (Fig. 8E); in contrast, faint staining of the stereocilia occurred in normal hair cells (Fig. 8B). In noise-damaged regions, distorted and condensed nuclei, as illustrated by propidium iodide (PI) labeling, were evident (Fig. 8F). The increase in the expression of FAK p-Tyr577 in stereocilia of noise-damaged hair cells is consistent with the noise-induced increase in the expression of this protein observed in the sensory epithelium using the antibody microarray.

WSTF immunoreactivity was detected in both the normal and noise damaged cochleae (Fig. 9). Strong signals appeared mainly in the stereocilia of OHC and IHC, OHC basal bodies, and in phalangeal processes of Deiters' cells. Major changes in the expression of WSTF following noise exposure appeared either in the stereocilia of damaged hair cells (arrows in Fig. 9D), or in the Deiters' cell adjacent to damaged hair cells (arrows in Figs. 9E and 9F) as evidenced by PI nuclear staining (data not shown). This increase in the expression of WSTF in the noise-damaged cochleae is consistent with the findings of the antibody microarray, which indicated an increase in the expression levels in the sensory epithelium after noise exposure. Collectively, these immunocytochemistry results not only support the findings of the antibody microarrays, but also revealed the distribution pattern of these proteins in the organ of Corti.

Immunoblotting of cochlear tissue enriched for nuclear proteins and plasma membrane proteins

To facilitate the validation of noise-induced changes in protein levels by immunoblotting methods, nuclear proteins and plasma membrane proteins from chinchilla cochleae were enriched (Fig. 10). The expression of WSTF and E2F3 was detected in this simple low speed pellet fraction. Noise induced a 1.7 fold increase in a 94 kDa WSTF-positive protein. The difference between the measured molecular weight for the cochlear protein and that detected for WSTF from cell cultures (170 kDa) suggests the possibility of a cochlear specific isoform. Alternatively, the findings may also be the result of proteolytic activity not encountered in previous studies of WSTF [40, 41]. Although, the E2F3 immunoblot showed multiple bands possibly due to different E2F family isoforms, the most prominent protein band at 61 kDa which migrates with the expected electrophoretic mobility for E2F3 (57 kDa) changed by 1.3 fold after noise exposure. In addition, a noise-induced 1.3 fold increase in Src was detected in the low speed pellet fraction. The expression levels of these proteins were normalized with the expression of actin.

Discussion

Noise exposure is a major cause of hearing loss and tinnitus among young adults. Previous gene expression studies have identified a host of genes that are significantly up-regulated and down-regulated with NIHL [42–44]. Although these gene expression studies provide important clues about the underlying mechanisms leading to NIHL and cochlear degeneration, it is unclear if the changes in genomic message are translated into a corresponding change in protein expression. While thousands of genes can be screened for change of expression in a matter of day or weeks, conventional tools for screening for changes in protein expression tend to be slower, less well developed and narrower in scope. The antibody microarray technique employed in the current study is a relatively high throughput method for simultaneously identifying changes in expression of more than 700 proteins. Because the antibodies are already available, any of the proteins (594 sensory epithelium, 392 lateral wall and 569 modiolus) identified on the arrays from normal or noise-exposed tissues (Supplementary Table 1) can then be localized to specific regions of the inner ear. The results presented here, the first high throughput protein analysis of NIHL, show that the early noise-induced proteomic responses differ significantly among the three

discrete regions of the cochlea. Noise induced an early increase in the expression of FAK p-Tyr577, E2F3, hMps1, serine threonine protein phosphatase 1b, activated p38/MAPK, WSTF and Fas in the sensory epithelium. In contrast, a decrease in protein expression was observed in E2F3, tropomyosin, CD146 and hnRNPA1 in the lateral wall. In the modiolus, a notable increase was observed in aurora B, BID, HDAC10 and ADAM17 while a decrease occurred in cytokeratin 8 12, PRMT1, serine threonine protein phosphatase 2 A/B, NG2, brain nitric oxide synthase, DEDAF and plakoglobin in the modiolus. Our subsequent experiments focused on the sensory epithelium because it contains the organ of Corti with the most vulnerable and critical cell types, the OHC and IHC. The involvement of nuclear proteins E2F3 and WSTF have not previously been reported in the stress response of the organ of Corti to noise or any other stimulus. Coupled with the detection of 2 proteins with posttranslational modifications (activated p38/MAPK and FAK phosphorylated on tyrosine 577) the noise-induced proteomic changes in the sensory epithelium support a mechanistic role for p38/MAPK signaling in noise-induced stress responses of the inner ear.

Sensory Epithelium Response

Our results identified important protein expression and posttranslational modifications during the very early stages of NIHL (2 h post exposure). The DPOAEs were abolished at this time confirming that the cochlea was severely traumatized when the protein assays were conducted. At the 2 h time point, seven proteins in the sensory epithelium met the selection criteria for large fold changes in expression (activated p38/MAPK, FAK p-Tyr577, Fas, hMps1 kinase, serine threonine protein phosphatase 1b, WSTF & E2F3). Our network analysis indicated that many of these proteins interact with one another. Evidence supporting an interaction among p38/MAPK, WSTF, E2F3, and phospho-FAK is provided by anatomical studies showing that all of these proteins are expressed in a common anatomical compartment, the OHC. Our immunolabeling results indicate that WSTF, E2F3 and FAK p-Tyr577 are expressed in OHC while previous studies showed immunolocalization of p38/MAPK in OHC [45]. Mechanistically, all of these proteins are known to interact with another signaling protein, Src, which has also been implicated in OHC viability in response to noise [46].

Focal adhesion signaling

FAK is a non-receptor protein-tyrosine kinase that regulates local signaling at adherens junctions, tight junctions and focal adhesions. FAK can also translocate to the nucleus to modulate transcription [47, 48]. In the control organ of Corti, we detected immunolabeling of FAK phosphorylated on tyrosine 577 in the nuclei of hair cells and supporting cells and in the phalangeal processes of pillar and Deiters' cells in the region of adhesion between hair cells and supporting cells (Fig. 8). This region, the reticular lamina, is known to be rich in both tight and adherens junctions [49]. In the noise exposed organ of Corti, FAK p-Tyr577 was also detected in OHC stereocilia, but only in noise damaged regions. Stereocilia are among the earliest hair cell organelles to show noise-induced morphological damage [50]. We speculate that excessive noise-induced mechanical stress of stereocilia induces FAK phosphorylation in stereocilia. FAK is known to be activated by extracellular mechanical forces exerted through focal adhesions, by phosphorylation of tyrosine 577, and by Src kinases that are associated with integrin signaling complexes [51]. FAK and alpha8beta1 integrin have previously been linked to normal stereocilia development [52]. Because of the critical role of stereocilia in cochlear function, the significance of observations of stimulus-induced posttranslational modifications in stereocilia proteins must ultimately stand up to rigorous testing. Nevertheless, we report data that suggests, for the first time, that phosphorylation of tyrosine 577 on FAK may be an early indicator of hair cell damage.

Phosphorylation of FAK on tyrosine 577 by Src increases its catalytic activity [53] whereas the phosphorylation of its serine residues leads to inactivation of FAK/integrin associated signaling [54]. The noise-induced increase in serine threonine protein phosphatase 1b (Ppp1cb) observed in our proteomic experiment may serve to maintain FAK in its active state as Ppp1cb has been reported to directly associate with FAK [55]. This type of activation of FAK-Src complexes is vital for downstream signaling pathways that control cell spreading, cell movement and cell survival. The regulation of p38/MAPK signaling via activated Rac is one such important pathway [18].

p38/MAPK signaling

p38/MAPK signaling is an important stress activated protein kinase pathway and is central to the observations of early noise-induced proteomic responses. Oxidative stress, which occurs during noise exposure [9], is known to up-regulate the Fas ligand that binds with the Fas (CD95/Apo1) receptor and leads to the formation of the death inducing signaling complex [56]. The noise-induced up-regulation of the Fas receptor is probably an important upstream event in NIHL as these receptors are known to mediate signaling cascades that ultimately lead to apoptosis through the activation of p38/MAPK [17]. The increase in the levels of diphosphorylated p38/MAPK is consistent with this hypothesis as p38/MAPK is a known downstream signaling molecule of Fas mediated apoptosis. Moreover, an upregulation of p38/MAPK has been reported in the acute phase of the PTS induced by acoustic trauma [57]. Hence, it seems likely that the p38/MAPK signaling pathway transduces noise-induced stress signals from the cell surface to the nucleus. Up-regulation of two downstream transcription factors (E2F3 and WSTF) that are associated with p38/MAPK signaling, after noise exposure, strengthens this speculation.

Apoptotic signals such as Fas can inactivate Rb through p38/MAPK pathway [58]. Rb inactivation itself can result in rapid cell-cycle reentry and death of hair cells [59]. In response to Rb inactivation, E2F3 can promote apoptosis [22]. Over-expression of E2F3 can induce ATM autophosphorylation which in turn phosphorylates p53 thereby promoting apoptosis [60]. This interpretation is consistent with previous studies showing up-regulation of phosphorylated p53 in response to ototoxic insults [61]. We interpret the noise-induced increase in E2F3 as an early indicator of apoptotic damage to the OHC. This role for E2F3 is supported by its striking up-regulation in OHC nuclei in regions damaged by noise. Immunoblotting confirmed the noise-induced increase of a 61 kDa protein in the nuclear and plasma membrane fraction consistent with a predicted molecular weight of 57 kDa for E2F3. Although the presence of other protein bands recognized by the antibody hampers this interpretation, it should be noted that prominent labeling is restricted to OHC nuclei (Fig 7) and the bands recognized by the antibody in immunoblot assays (Fig. 10) are consistent with the range of molecular weights of other members of the E2F family of transcription factors. Results for p38/MAPK and E2F3 predict that noise will induce phosphorylation of Rb, its subsequent release from E2F transcription factors and transcription of E2F target genes. Future studies should test this prediction and confirm the proteomic and immunofluorescence results with more specific E2F antibodies.

Noise also induced an increase in WSTF levels in the sensory epithelium. MAPK dependent phosphorylation of WSTF plays an important role DNA repair mechanisms associated with the chromatin remodeling complex WINAC [21]. Higher expression of WSTF in the nuclear and plasma membrane extracts along with the increased signals observed in cells adjacent to the noise damaged regions of the organ of Corti suggest that activation of WSTF mediated repair mechanism may limit the damage caused by the noise insult. However, the lack of immunofluorescence signal from hair cell nuclei, despite the increases observed by immunoblotting and microarray assays, suggests the possibility that this transcription factor

and chromatin remodeling protein may have additional non-nuclear functions not previously reported.

The noise-induced increase in hMps1 kinase (Ttk), a critical mitotic checkpoint protein, is also consistent with apoptotic damage since Ttk expression after DNA damage contributes to apoptosis [62]. Collectively, the functional role of Ttk, WSTF, E2F3, Ppp1cb, Fas, p38/MAPK and FAK as well as their interactions determined by bioinformatic analysis of the noise-induced proteomic responses suggest the initiation of the cell death process in the sensory epithelium. These observations extend previous reports from our group of apoptosis occurring as early as 5 min after noise exposure [63].

Lateral Wall Response

A relatively small number of proteins in lateral wall tissue showed significant changes in expression after the exposure. Noise induced a decrease in E2F3, hnRNPA1, tropomyosin and an endothelial cell marker protein that recognizes membrane protein CD146. E2F3 is known to play an important role in controlling the cell cycle and apoptosis which implies that the noise-induced decrease in E2F3 is likely to affect the cell cycle regulation and cell death in lateral wall. hnRNPA1, a heterogeneous nuclear ribonucleoprotein is associated with processing and export of mRNA from the nucleus. Noise-induced decrease in hnRNPA1 assumes greater significance due to the role of hnRNPs in regulating repair and stress response mRNAs [64]. We speculate that the noise exposure could impair the regulation of mRNAs associated with the stress response in the lateral wall by decreasing the levels of hnRNPA1. Decreased levels of CD 146, a membrane glycoprotein that functions as a Ca^{2+}-independent cell adhesion molecule [65] may be a biomarker for shear stress resulting from a noise-induced increase in cochlear blood flow [66] in the stria vascularis. Tropomyosin could also contribute to noise-induced shear stress as removal of tropomyosin from its actin binding site facilitates myosin binding with actin leading to muscle contraction [67].

Modiolar Response

Noise induced a variety of protein expression changes in the modiolus many of which were associated with apoptosis. This is consistent with a previous report indicating the early onset of damage to spiral ganglion neurons after acoustic stimulation [68]. Known functional roles of 7 proteins that decreased in the modiolus suggest that, 2 proteins reflect a cell death response, 3 proteins reflect a survival response while the remaining 2 have varied functions. Noise-induced decrease in NG2 and DEDAF suggest an apoptotic response. The decrease in NG2, a chondroitin sulfate proteoglycan 4 found in the nervous system, can inhibit axon growth and has been associated with wound healing [69]. DEDAF is death effector domain-associated factor that interacts with DEDs in proteins that regulate programmed cell death. A decrease in DEDAF may indicate an attempt to maintain cellular homeostasis in the face of noise-induced apoptosis where the DED containing proteins are trying to establish a cell renewal point to co-regulate proliferation and apoptosis [70]. The noise-induced decrease in gamma-catenin, serine threonine protein phosphatase 2A and nitric oxide synthase (bNOS) suggest a survival response. The deficiency of gamma-catenin (plakoglobin), a tumor suppressor present at cell adhesion sites [71], has been reported to result in an increase in Bcl-X(L) and confer protection from apoptosis [72]. Serine threonine protein phosphatase 2A is implicated in the negative control of cell growth and division [73] while nitric oxide synthase enzyme catalyzes the production of nitric oxide which mediates various functions including nitration of proteins, which has been reported as a marker of neuronal degeneration [74]. Apart from these, protein arginine methyltransferase 1 is a histone methyltransferase important for signal transduction, transcription, RNA transport, and splicing [75] while cytokeratins are intermediate filament proteins responsible for the

structural integrity of epithelial cells. Among the 4 proteins that increased, the nuclear protein aurora kinase B is a key regulator for the onset of cytokinesis during mitosis [76]. Adam metallopeptidase domain 17, a tumor necrosis factor-alpha converting enzyme, has a prominent role in the activation of the Notch signaling pathway [77]. The increase of ADAM17 in the neuronal tissue of cochlea suggests that noise activates notch signaling, which has an important role in neuronal function and development [78]. Histone deacetylase 10 (HDAC10) is responsible for deacetylation of lysine residues on histones and presumably on cytoplasmic substrates [79]. The biology of HDAC10 activity is largely unexplored, however, it has recently been shown to interact with and regulate Pax3 [80] a transcription factor which when mutated can result in congenital hearing loss associated with Waardenburg syndrome types I and III [81]. The noise-induced increase in Bid, which is a BH3 interacting domain death agonist, indicates the up-regulation of apoptotic responses in modiolus as it is a member of the BCL-2 family of cell death regulators that mediates mitochondrial damage induced by caspase-8 [82]. Collectively, the noise-induced changes and the functional roles of many, if not all, of these proteins indicate the predominance of an apoptotic response in the modiolus.

Conclusions

Overall, this first large scale proteomic study of noise induced damage to the inner ear, indicates that the noise-induced proteomic responses of the three discrete regions of the inner ear differ at an early stage after noise. Noise exposure induced an apoptotic response in the sensory epithelium and modiolus while the responses in the lateral wall were more limited. Bioinformatic analysis suggested the involvement of Fas, focal adhesion and MAPK signaling pathways in the initiation of the cell death process in the sensory epithelium. The noise-induced changes in cochlear proteins, including certain posttranslational modifications (e.g., phosphorylation of FAK and p38/MAPK), from different subcellular regions of the sensory epithelium revealed new aspects of the pivotal role p38/MAPK signaling plays in the molecular mechanisms underlying NIHL. In addition, we measured relative expression levels in around 500 proteins in each of the three tissue compartments; these data provide the first comprehensive profile of the proteins located in each of these unique tissue compartments. Finally, we identified several novel proteins associated with NIHL which may provide new clues regarding the mechanism underlying cell death and survival in the inner ear following noise-exposure. Proteomic analysis at later time points may further clarify the downstream events in other cochlear regions.

Supplementary Material

Refer to Web version on PubMed Central for supplementary material.

Acknowledgments

We thank Daniel Stolzberg for helping us to set up the noise exposure device. This study was supported by National Institutes of Health/NIDCD Grants R03DC010225, SJ; R01DC009091 & 1R01DC009219, RS.

Abbreviations

NIHL	noise induced hearing loss
dB	decibel
SPL	sound pressure level
MAPK	mitogen activated protein kinase

WSTF	Williams syndrome transcription factor
IHC	inner hair cells
OHC	outer hair cells
SGN	spiral ganglion neurons
DPOAE	distortion product otoacoustic emission
DAVID	Database for Annotation, Visualization and Integrated Discovery
FAK	focal adhesion kinase
DEDAF	death effector domain-associated factor
Rb	retinoblastoma protein
PI	propidium iodide
PTS	permanent threshold shift
ATM	ataxia telangiectasia mutated

References

1. Nelson DI, Nelson RY, Concha-Barrientos M, Fingerhut M. The global burden of occupational noise-induced hearing loss. Am J Ind Med. 2005; 48:446–58. [PubMed: 16299704]
2. Cave KM, Cornish EM, Chandler DW. Blast injury of the ear: clinical update from the global war on terror. Mil Med. 2007; 172:726–30. [PubMed: 17691685]
3. Prazma J, Rodgers GK, Pillsbury HC. Cochlear blood flow. Effect of noise. Arch Otolaryngol. 1983; 109:611–5. [PubMed: 6882271]
4. Yamane H, Nakai Y, Konishi K, Sakamoto H, Matsuda Y, Iguchi H. Strial circulation impairment due to acoustic trauma. Acta Otolaryngol. 1991; 111:85–93. [PubMed: 2014760]
5. Jacono AA, Hu B, Kopke RD, Henderson D, Van De Water TR, Steinman HM. Changes in cochlear antioxidant enzyme activity after sound conditioning and noise exposure in the chinchilla. Hear Res. 1998; 117:31–8. [PubMed: 9557976]
6. Salvi RJ, Hamernik RP, Henderson D. Auditory nerve activity and cochlear morphology after noise exposure. Arch Otorhinolaryngol. 1979; 224:111–6. [PubMed: 485937]
7. Wang Y, Hirose K, Liberman MC. Dynamics of noise-induced cellular injury and repair in the mouse cochlea. J Assoc Res Otolaryngol. 2002; 3:248–68. [PubMed: 12382101]
8. Cheng AG, Cunningham LL, Rubel EW. Mechanisms of hair cell death and protection. Curr Opin Otolaryngol Head Neck Surg. 2005; 13:343–8. [PubMed: 16282762]
9. Henderson D, Bielefeld EC, Harris KC, Hu BH. The role of oxidative stress in noise-induced hearing loss. Ear Hear. 2006; 27:1–19. [PubMed: 16446561]
10. Nicotera TM, Hu BH, Henderson D. The caspase pathway in noise-induced apoptosis of the chinchilla cochlea. J Assoc Res Otolaryngol. 2003; 4:466–77. [PubMed: 14534835]
11. Van De Water TR, Lallemend F, Eshraghi AA, Ahsan S, He J, Guzman J, et al. Caspases, the enemy within, and their role in oxidative stress-induced apoptosis of inner ear sensory cells. Otol Neurotol. 2004; 25:627–32. [PubMed: 15241246]
12. Murai N, Kirkegaard M, Jarlebark L, Risling M, Suneson A, Ulfendahl M. Activation of JNK in the inner ear following impulse noise exposure. J Neurotrauma. 2008; 25:72–7. [PubMed: 18355160]
13. Salvi, R.; Sun, W.; Lobarinas, E. Anatomy and physiology of the peripheral auditory system. Thieme; New York: 2007.
14. Hu BH, Henderson D, Nicotera TM. Involvement of apoptosis in progression of cochlear lesion following exposure to intense noise. Hear Res. 2002; 166:62–71. [PubMed: 12062759]

15. Bohne BA, Harding GW, Lee SC. Death pathways in noise-damaged outer hair cells. Hear Res. 2007; 223:61–70. [PubMed: 17141990]
16. Coulthard LR, White DE, Jones DL, McDermott MF, Burchill SA. p38(MAPK): stress responses from molecular mechanisms to therapeutics. Trends Mol Med. 2009; 15:369–79. [PubMed: 19665431]
17. Juo P, Kuo CJ, Reynolds SE, Konz RF, Raingeaud J, Davis RJ, et al. Fas activation of the p38 mitogen-activated protein kinase signalling pathway requires ICE/CED-3 family proteases. Mol Cell Biol. 1997; 17:24–35. [PubMed: 8972182]
18. Philips A, Roux P, Coulon V, Bellanger JM, Vie A, Vignais ML, et al. Differential effect of Rac and Cdc42 on p38 kinase activity and cell cycle progression of nonadherent primary mouse fibroblasts. J Biol Chem. 2000; 275:5911–7. [PubMed: 10681583]
19. Tabuchi K, Oikawa K, Hoshino T, Nishimura B, Hayashi K, Yanagawa T, et al. Cochlear protection from acoustic injury by inhibitors of p38 mitogen-activated protein kinase and sequestosome 1 stress protein. Neuroscience. 2010; 166:665–70. [PubMed: 20036720]
20. Wei X, Zhao L, Liu J, Dodel RC, Farlow MR, Du Y. Minocycline prevents gentamicin-induced ototoxicity by inhibiting p38 MAP kinase phosphorylation and caspase 3 activation. Neuroscience. 2005; 131:513–21. [PubMed: 15708492]
21. Oya H, Yokoyama A, Yamaoka I, Fujiki R, Yonezawa M, Youn MY, et al. Phosphorylation of Williams syndrome transcription factor by MAPK induces a switching between two distinct chromatin remodeling complexes. J Biol Chem. 2009; 284:32472–82. [PubMed: 19776015]
22. Ziebold U, Reza T, Caron A, Lees JA. E2F3 contributes both to the inappropriate proliferation and to the apoptosis arising in Rb mutant embryos. Genes Dev. 2001; 15:386–91. [PubMed: 11230146]
23. Vicente-Torres MA, Schacht J. A BAD link to mitochondrial cell death in the cochlea of mice with noise-induced hearing loss. J Neurosci Res. 2006; 83:1564–72. [PubMed: 16521126]
24. Yamashita D, Minami SB, Kanzaki S, Ogawa K, Miller JM. Bcl-2 genes regulate noise-induced hearing loss. J Neurosci Res. 2008; 86:920–8. [PubMed: 17943992]
25. Jamesdaniel S, Ding D, Kermany MH, Davidson BA, Knight PR 3rd, Salvi R, et al. Proteomic analysis of the balance between survival and cell death responses in cisplatin-mediated ototoxicity. J Proteome Res. 2008; 7:3516–24. [PubMed: 18578524]
26. Jamesdaniel S, Ding D, Kermany MH, Jiang H, Salvi R, Coling D. Analysis of cochlear protein profiles of Wistar, Sprague-Dawley, and Fischer 344 rats with normal hearing function. J Proteome Res. 2009; 8:3520–8. [PubMed: 19432484]
27. Hamernik RP, Henderson D, Coling D, Salvi R. Influence of vibration on asymptotic threshold shift produced by impulse noise. Audiology. 1981; 20:259–69. [PubMed: 7213211]
28. Henderson D, Salvi RJ, Hamernik RP. Is the equal energy rule applicable to impact noise? Scand Audiol Suppl. 1982; 16:71–82. [PubMed: 6962515]
29. Salvi RJ, Hamernik RP, Henderson D. Discharge patterns in the cochlear nucleus of the chinchilla following noise induced asymptotic threshold shift. Exp Brain Res. 1978; 32:301–20. [PubMed: 680046]
30. Clock Eddins A, Zuskov M, Salvi RJ. Changes in distortion-product otoacoustic emissions in chinchillas with increasing levels of noise-induced asymptotic threshold shift. Ear and hearing. 1997
31. Durrant JD, Wang J, Ding DL, Salvi RJ. Are inner or outer hair cells the source of summating potentials recorded from the round window? J Acoust Soc Am. 1998; 104:370–7. [PubMed: 9670530]
32. Ding, DMS.; Salvi, RJ. Cochlear hair cell densities and inner ear staining techniques. In: Willott, JF., editor. The Auditory Psychobiology of the Mouse. Boca Raton, FL: CRC Press; 2001. p. 189-204.
33. Greenwood DD. A cochlear frequency-position function for several species--29 years later. J Acoust Soc Am. 1990; 87:2592–605. [PubMed: 2373794]
34. Bradford MM. A rapid and sensitive method for the quantitation of microgram quantities of protein utilizing the principle of protein-dye binding. Anal Biochem. 1976; 72:248–54. [PubMed: 942051]

35. Coling DE, Ding D, Young R, Lis M, Stofko E, Blumenthal KM, et al. Proteomic analysis of cisplatin-induced cochlear damage: methods and early changes in protein expression. Hear Res. 2007; 226:140–56. [PubMed: 17321087]
36. Huang da W, Sherman BT, Lempicki RA. Systematic and integrative analysis of large gene lists using DAVID bioinformatics resources. Nat Protoc. 2009; 4:44–57. [PubMed: 19131956]
37. Coling DE, Espreafico EM, Kachar B. Cellular distribution of myosin-V in the guinea pig cochlea. J Neurocytol. 1997; 26:113–20. [PubMed: 9181485]
38. Widnell CC, Tata JR. A procedure for the isolation of enzymically active rat-liver nuclei. Biochem J. 1964; 92:313–7. [PubMed: 4284460]
39. Coling DE, Naik RM, Schacht J. Calcium and calmodulin inhibit phosphorylation of a novel auditory nerve protein. Hear Res. 1994; 72:197–205. [PubMed: 7512086]
40. Cavellan E, Asp P, Percipalle P, Farrants AK. The WSTF-SNF2h chromatin remodeling complex interacts with several nuclear proteins in transcription. J Biol Chem. 2006; 281:16264–71. [PubMed: 16603771]
41. Xiao A, Li H, Shechter D, Ahn SH, Fabrizio LA, Erdjument-Bromage H, et al. WSTF regulates the H2A.X DNA damage response via a novel tyrosine kinase activity. Nature. 2009; 457:57–62. [PubMed: 19092802]
42. Cho Y, Gong TW, Kanicki A, Altschuler RA, Lomax MI. Noise overstimulation induces immediate early genes in the rat cochlea. Brain Res Mol Brain Res. 2004; 130:134–48. [PubMed: 15519684]
43. Kirkegaard M, Murai N, Risling M, Suneson A, Jarlebark L, Ulfendahl M. Differential gene expression in the rat cochlea after exposure to impulse noise. Neuroscience. 2006; 142:425–35. [PubMed: 16887274]
44. Hu BH, Cai Q, Manohar S, Jiang H, Ding D, Coling DE, et al. Differential expression of apoptosis-related genes in the cochlea of noise-exposed rats. Neuroscience. 2009; 161:915–25. [PubMed: 19348871]
45. Sha SH, Chen FQ, Schacht J. Activation of cell death pathways in the inner ear of the aging CBA/J mouse. Hear Res. 2009; 254:92–9. [PubMed: 19422898]
46. Harris KC, Hu B, Hangauer D, Henderson D. Prevention of noise-induced hearing loss with Src-PTK inhibitors. Hear Res. 2005; 208:14–25. [PubMed: 15950415]
47. Almeida EA, Ilic D, Han Q, Hauck CR, Jin F, Kawakatsu H, et al. Matrix survival signaling: from fibronectin via focal adhesion kinase to c-Jun NH(2)-terminal kinase. J Cell Biol. 2000; 149:741–54. [PubMed: 10791986]
48. Ilic D, Almeida EA, Schlaepfer DD, Dazin P, Aizawa S, Damsky CH. Extracellular matrix survival signals transduced by focal adhesion kinase suppress p53-mediated apoptosis. J Cell Biol. 1998; 143:547–60. [PubMed: 9786962]
49. Gulley RL, Reese TS. Intercellular junctions in the reticular lamina of the organ of Corti. J Neurocytol. 1976; 5:479–507. [PubMed: 993823]
50. Liberman MC, Dodds LW. Acute ultrastructural changes in acoustic trauma: serial-section reconstruction of stereocilia and cuticular plates. Hear Res. 1987; 26:45–64. [PubMed: 3558143]
51. Wang Y, Botvinick EL, Zhao Y, Berns MW, Usami S, Tsien RY, et al. Visualizing the mechanical activation of Src. Nature. 2005; 434:1040–5. [PubMed: 15846350]
52. Littlewood Evans A, Muller U. Stereocilia defects in the sensory hair cells of the inner ear in mice deficient in integrin alpha8beta1. Nat Genet. 2000; 24:424–8. [PubMed: 10742111]
53. Maa MC, Leu TH. Vanadate-dependent FAK activation is accomplished by the sustained FAK Tyr-576/577 phosphorylation. Biochem Biophys Res Commun. 1998; 251:344–9. [PubMed: 9790958]
54. Yamakita Y, Totsukawa G, Yamashiro S, Fry D, Zhang X, Hanks SK, et al. Dissociation of FAK/p130(CAS)/c-Src complex during mitosis: role of mitosis-specific serine phosphorylation of FAK. J Cell Biol. 1999; 144:315–24. [PubMed: 9922457]
55. Fresu M, Bianchi M, Parsons JT, Villa-Moruzzi E. Cell-cycle-dependent association of protein phosphatase 1 and focal adhesion kinase. Biochem J. 2001; 358:407–14. [PubMed: 11513739]
56. Suzuki M, Aoshiba K, Nagai A. Oxidative stress increases Fas ligand expression in endothelial cells. J Inflamm (Lond). 2006; 3:11. [PubMed: 16854215]

57. Meltser I, Tahera Y, Canlon B. Differential activation of mitogen-activated protein kinases and brain-derived neurotrophic factor after temporary or permanent damage to a sensory system. Neuroscience. 2010; 165:1439–46. [PubMed: 19925854]
58. Wang S, Nath N, Minden A, Chellappan S. Regulation of Rb and E2F by signal transduction cascades: divergent effects of JNK1 and p38 kinases. Embo J. 1999; 18:1559–70. [PubMed: 10075927]
59. Weber T, Corbett MK, Chow LM, Valentine MB, Baker SJ, Zuo J. Rapid cell-cycle reentry and cell death after acute inactivation of the retinoblastoma gene product in postnatal cochlear hair cells. Proc Natl Acad Sci U S A. 2008; 105:781–5. [PubMed: 18178626]
60. Hong S, Paulson QX, Johnson DG. E2F1 and E2F3 activate ATM through distinct mechanisms to promote E1A-induced apoptosis. Cell Cycle. 2008; 7:391–400. [PubMed: 18235226]
61. Zhang M, Liu W, Ding D, Salvi R. Pifithrin-alpha suppresses p53 and protects cochlear and vestibular hair cells from cisplatin-induced apoptosis. Neuroscience. 2003; 120:191–205. [PubMed: 12849752]
62. Bhonde MR, Hanski ML, Budczies J, Cao M, Gillissen B, Moorthy D, et al. DNA damage-induced expression of p53 suppresses mitotic checkpoint kinase hMps1: the lack of this suppression in p53MUT cells contributes to apoptosis. J Biol Chem. 2006; 281:8675–85. [PubMed: 16446370]
63. Hu BH, Henderson D, Nicotera TM. Extremely rapid induction of outer hair cell apoptosis in the chinchilla cochlea following exposure to impulse noise. Hear Res. 2006; 211:16–25. [PubMed: 16219436]
64. Haley B, Paunesku T, Protic M, Woloschak GE. Response of heterogeneous ribonuclear proteins (hnRNP) to ionising radiation and their involvement in DNA damage repair. Int J Radiat Biol. 2009; 85:643–55. [PubMed: 19579069]
65. Solovey A, Lin Y, Browne P, Choong S, Wayner E, Hebbel RP. Circulating activated endothelial cells in sickle cell anemia. N Engl J Med. 1997; 337:1584–90. [PubMed: 9371854]
66. Prazma J, Vance SG, Bolster DE, Pillsbury HC, Postma DS. Cochlear blood flow. The effect of noise at 60 minutes' exposure. Arch Otolaryngol Head Neck Surg. 1987; 113:36–9. [PubMed: 3790282]
67. Marston S, El-Mezgueldi M. Role of tropomyosin in the regulation of contraction in smooth muscle. Adv Exp Med Biol. 2008; 644:110–23. [PubMed: 19209817]
68. Chen Z, Peppi M, Kujawa SG, Sewell WF. Regulated expression of surface AMPA receptors reduces excitotoxicity in auditory neurons. J Neurophysiol. 2009; 102:1152–9. [PubMed: 19515954]
69. Tan AM, Colletti M, Rorai AT, Skene JH, Levine JM. Antibodies against the NG2 proteoglycan promote the regeneration of sensory axons within the dorsal columns of the spinal cord. J Neurosci. 2006; 26:4729–39. [PubMed: 16672645]
70. Tibbetts MD, Zheng L, Lenardo MJ. The death effector domain protein family: regulators of cellular homeostasis. Nat Immunol. 2003; 4:404–9. [PubMed: 12719729]
71. Winn RA, Bremnes RM, Bemis L, Franklin WA, Miller YE, Cool C, et al. gamma-Catenin expression is reduced or absent in a subset of human lung cancers and re-expression inhibits transformed cell growth. Oncogene. 2002; 21:7497–506. [PubMed: 12386812]
72. Dusek RL, Godsel LM, Chen F, Strohecker AM, Getsios S, Harmon R, et al. Plakoglobin deficiency protects keratinocytes from apoptosis. J Invest Dermatol. 2007; 127:792–801. [PubMed: 17110936]
73. Janssens V, Goris J. Protein phosphatase 2A: a highly regulated family of serine/threonine phosphatases implicated in cell growth and signalling. Biochem J. 2001; 353:417–39. [PubMed: 11171037]
74. Abe K, Pan LH, Watanabe M, Konno H, Kato T, Itoyama Y. Upregulation of protein-tyrosine nitration in the anterior horn cells of amyotrophic lateral sclerosis. Neurol Res. 1997; 19:124–8. [PubMed: 9175139]
75. Rho J, Choi S, Seong YR, Choi J, Im DS. The arginine-1493 residue in QRRGRTGR1493G motif IV of the hepatitis C virus NS3 helicase domain is essential for NS3 protein methylation by the protein arginine methyltransferase 1. J Virol. 2001; 75:8031–44. [PubMed: 11483748]

76. Andrews PD, Knatko E, Moore WJ, Swedlow JR. Mitotic mechanics: the auroras come into view. Curr Opin Cell Biol. 2003; 15:672–83. [PubMed: 14644191]

77. Bozkulak EC, Weinmaster G. Selective use of ADAM10 and ADAM17 in activation of Notch1 signaling. Mol Cell Biol. 2009; 29:5679–95. [PubMed: 19704010]

78. Gaiano N, Fishell G. The role of notch in promoting glial and neural stem cell fates. Annu Rev Neurosci. 2002; 25:471–90. [PubMed: 12052917]

79. Kao HY, Lee CH, Komarov A, Han CC, Evans RM. Isolation and characterization of mammalian HDAC10, a novel histone deacetylase. J Biol Chem. 2002; 277:187–93. [PubMed: 11677242]

80. Lai IL, Lin TP, Yao YL, Lin CY, Hsieh MJ, Yang WM. Histone deacetylase 10 relieves repression on the melanogenic program by maintaining the deacetylation status of repressors. J Biol Chem. 2010; 285:7187–96. [PubMed: 20032463]

81. Pingault V, Ente D, Dastot-Le Moal F, Goossens M, Marlin S, Bondurand N. Review and update of mutations causing Waardenburg syndrome. Hum Mutat. 2010; 31:391–406. [PubMed: 20127975]

82. Li H, Zhu H, Xu CJ, Yuan J. Cleavage of BID by caspase 8 mediates the mitochondrial damage in the Fas pathway of apoptosis. Cell. 1998; 94:491–501. [PubMed: 9727492]

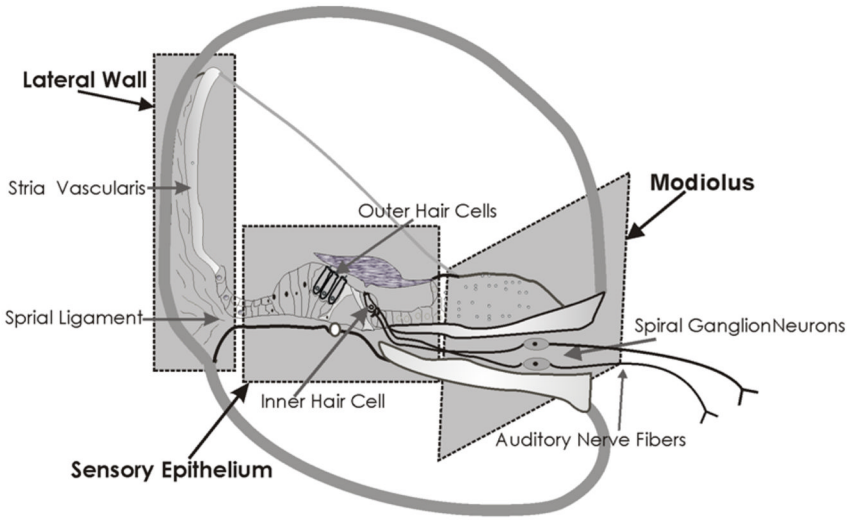

Figure 1. Schematic of the Cochlea

The schematic illustrates the complex structure of the cochlea. The different cellular types included in the three discrete regions used for proteomic screening have been highlighted with dotted lines in this section of the cochlea.

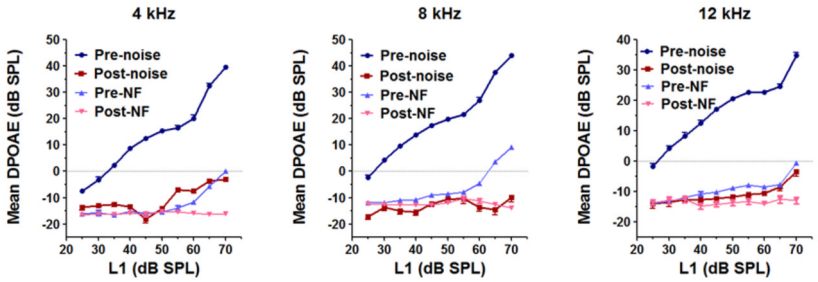

Figure 2. Hearing loss at 2h after noise exposure

DPOAEs recorded before and after noise exposure at f2 frequencies 4, 8 & 12 kHz for ten animals subjected to proteomic screening indicate that exposure to 0.5 – 8 kHz noise at 112 dB SPL for 2 h induced a significant decrease in the DPOAE amplitudes at 2h after noise exposure. The results are expressed as mean ± standard error, n = 10. The traces pre- and post- NF are the noise floor levels of the DPOAE recordings done before and after noise exposure.

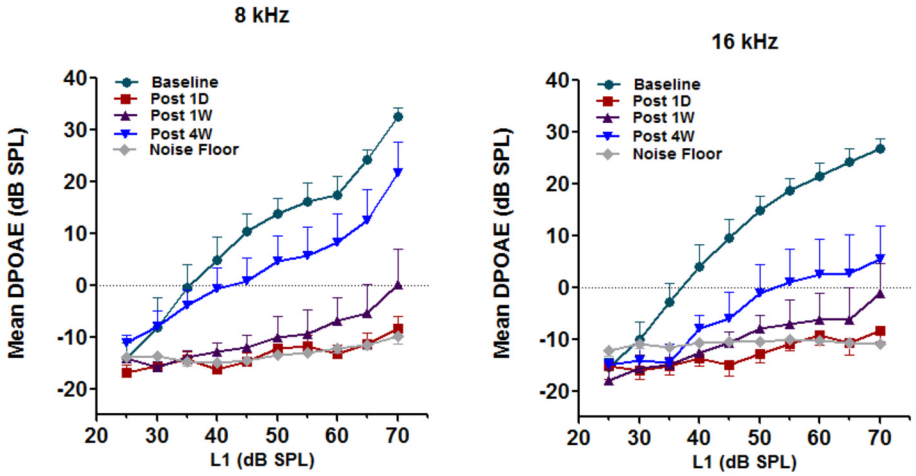

Figure 3. Noise-induced permanent threshold shift

DPOAEs recorded in three animals before and 1 day, 7days and 28 days after noise exposure indicate a shift in the permanent hearing threshold. The distortion product amplitudes at f2 frequency 8 kHz and 16 kHz showed a mild recovery 7 days after noise exposure and a moderate recovery after 28 days. Nevertheless, the amplitude was 10 to 20 dB lower than the pre exposure levels. The results are expressed as mean ± standard error, n = 3.

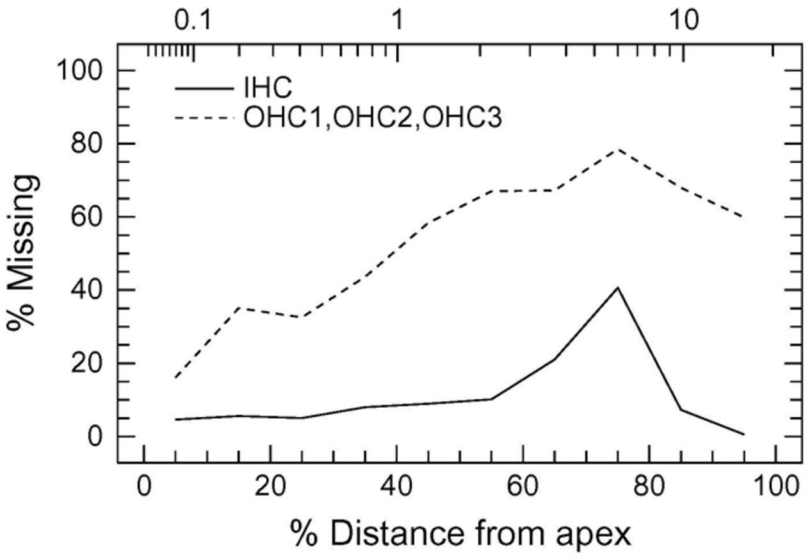

Figure 4. Hair cell loss after noise exposure

Cochleograms were recorded 28 days after 112dB broad band noise exposure for 2 hours (centered at 0.5–8.0 kHz). A massive loss of outer hair cells was observed in the basal region with widespread loss in the middle turn and moderate loss towards the apex. The inner hair cells indicated a 40% loss in the region expected for the noise while adjoining areas on both sides had a small to moderate loss. Cochleograms recorded in 3 animals were averaged.

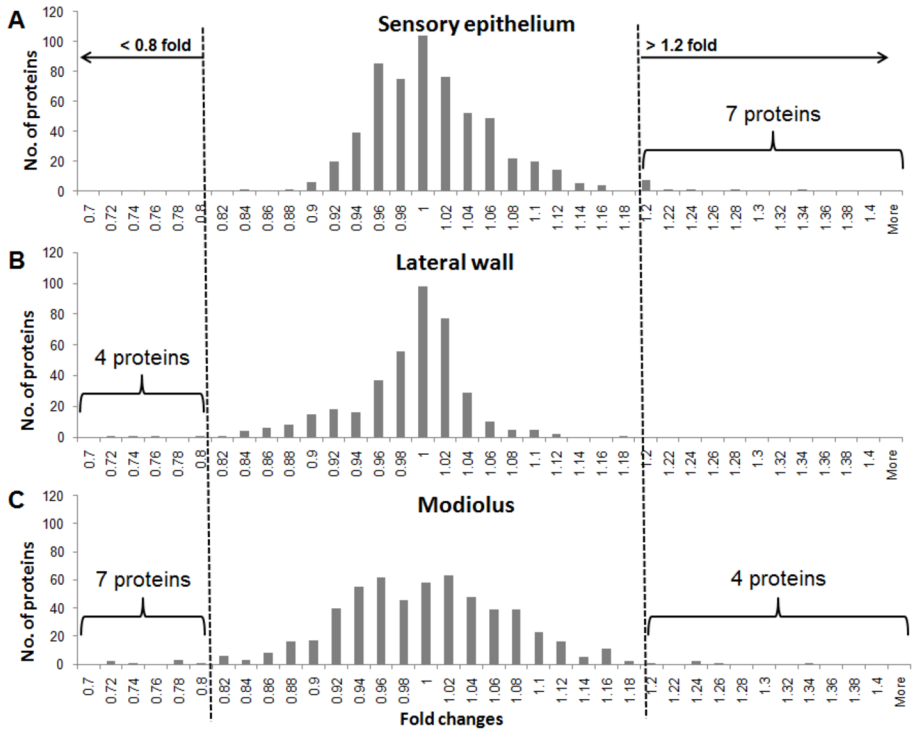

Figure 5. Protein profile in three discrete regions of the cochlea after noise exposure

The protein expression profile of the sensory epithelium, lateral wall and modiolus plots the number of proteins (Y axis) versus the fold changes (X axis). These graphical illustrations suggest that the noise-induced changes follow a normal pattern of distribution in the A) sensory epithelium, B) lateral wall and C) modiolus of chinchilla cochlea. Proteins that change by a value greater than 1 indicate a noise induced increase while those that change by a value less than 1 indicate a decrease.

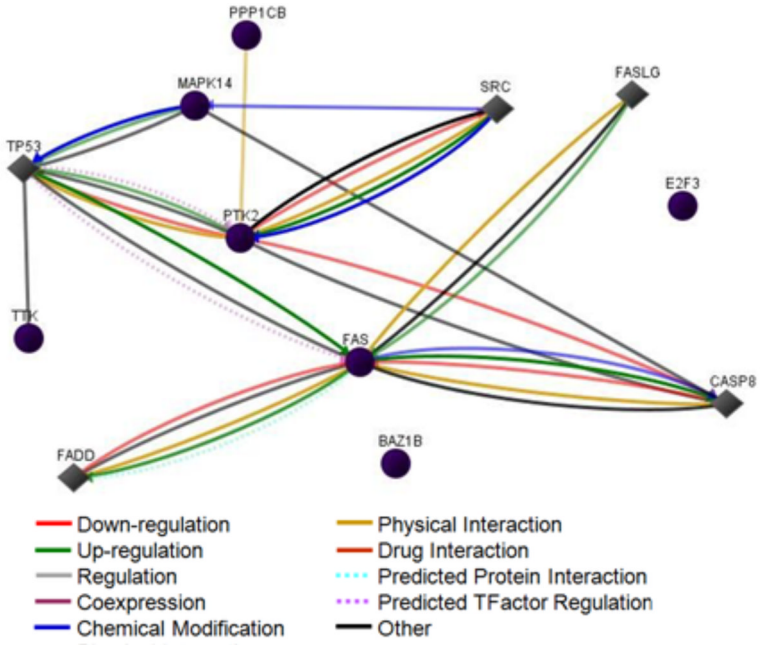

Figure 6. Network analysis of noise-induced proteomic changes in sensory epithelium

Network analysis by SABiosciences GNCPro software indicated that most of the proteins that changed in the sensory epithelium were involved in a network that also included Src and suggested that these proteins had biochemical as well as physical interactions. Circles represent the originally analyzed proteins while diamonds represent those that were added to the network during a one step expansion. Gene symbols are used to indicate the proteins.

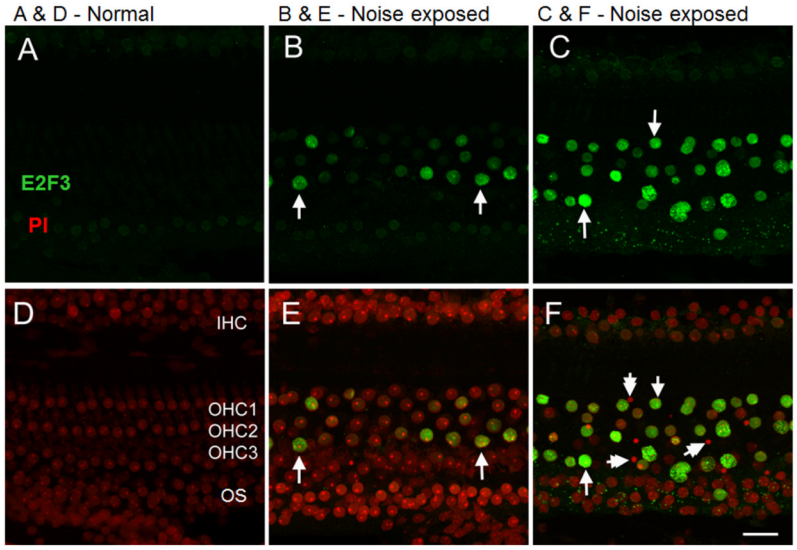

Figure 7. Immunolocalization of E2F3 in the organ of Corti

Panels A and D illustrate E2F3 staining in a normal cochlea. B and E show the staining in a section of the organ of Corti adjacent to the severely-damaged section from a noise-traumatized cochlea. Even though there are no condensed nuclei in this region, certain nuclei display E2F3 immunoreactivity. C and F show a severely-damaged section of the organ of Corti from the second cochlear turn. The arrows point to the nuclei having strong E2F3 immunoreactivity. The double-arrows point to the condensed nuclei that lack E2F3 fluorescence. The panels show the inner hair cells (IHC), three rows of outer hair cells (OHC) and supporting cells from the outer sulcus (OS). Green staining indicates E2F3 while red (propidium iodide) indicates nuclear staining. Bar = 21 μm.

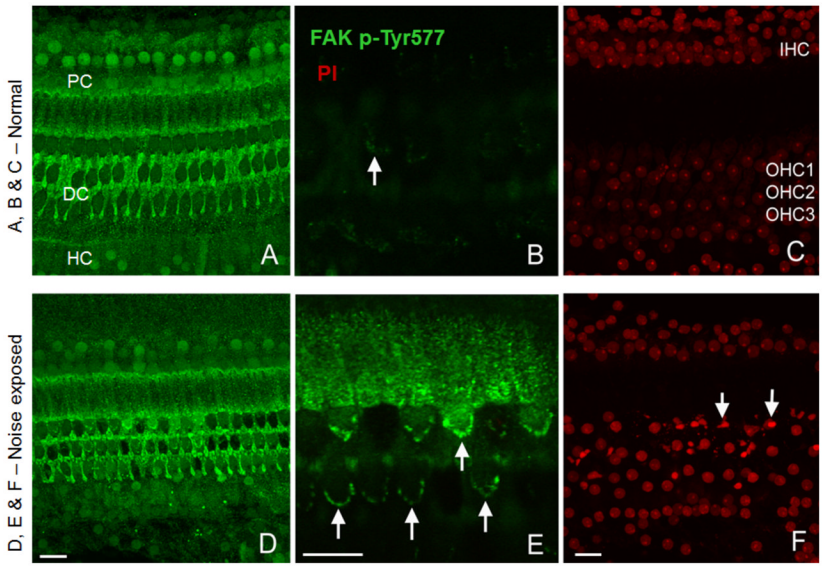

Figure 8. Immunolocalization of FAK p-Tyr577 in the organ of Corti

Panels A, B and C show a normal cochlear section. D, E and F show a section displaying severe HC damage. Confocal images at the level of stereocilia (B and E) illustrates the major difference between the normal and the noise damaged cochleae, with strong signals (Green) from the stereocilia of noise exposed animals. The pillar cells (PC), Deiters' cells (DC), Hensen's cells (HC) are shown in the images along with the inner and outer hair cells (IHC & OHC). Bar = 17 μm. Note panels B and E have a higher magnification.

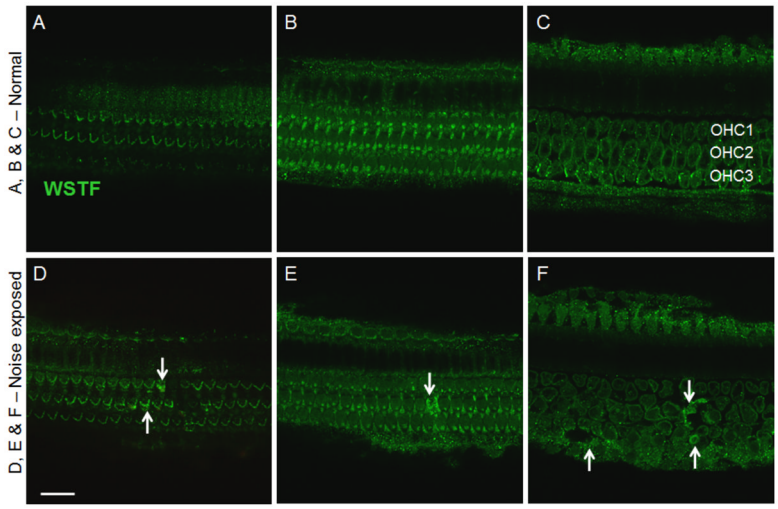

Figure 9. Immunolocalization of WSTF in the organ of Corti

Panels A, B and C show a normal cochlear section. D, E and F show a section displaying noise induced hair cell damage. Confocal images at the level of stereocilia (A and D) illustrates that stereocilia adjacent to the noise damaged region (D) indicated by arrows show strong signals (Green). Images at the level of cuticular plate (B and E) and the body of OHC (C and F) also indicate a similar pattern displaying increased WSTF immunoreactivity (shown by arrows) in regions adjoining the noise damaged cells. Bar = 20 μm.

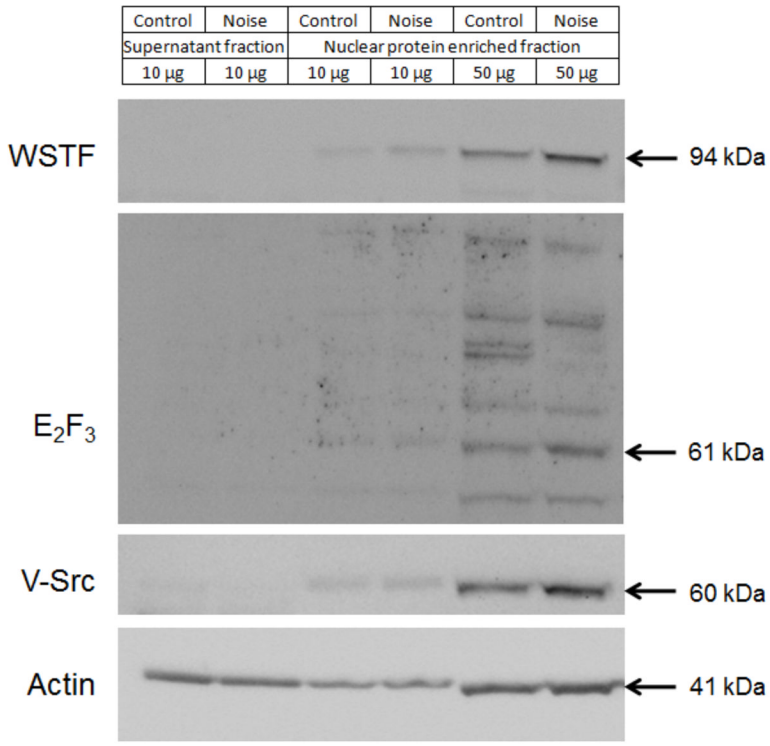

Figure 10. Immunoblotting of nuclear protein enriched fraction

Noise-induced increases in nuclear proteins were verified by immunoblotting a nuclear fraction of cochlear protein extract. A 1.7 fold increase was detected for a single WSTF-positive protein. E2F3 showed multiple bands possibly due to different E2F gene products while a 61 kDa protein, which is close to the predicted molecular weight changed by 1.3 fold. Noise also induced a 1.3 fold increase in Src protein. The images were cropped to show the particular bands as except for E2F3 all other proteins were specific. Actin was used to normalize the protein expression levels. The images are representative samples from two replicates.